Journal of Nanobiotechnology

RESEARCH Open Access

Lacc1-engineered extracellular vesicles reprogram mitochondrial metabolism to alleviate inflammation and cartilage degeneration in TMJ osteoarthritis

Xiaofeng Hu[1], Jian Xie[1*] and Jiansheng Su[1*]

Abstract

Temporomandibular joint osteoarthritis (TMJOA) is a multifaceted degenerative disease characterized by progressive cartilage degradation, chronic pain, and functional limitations of the TMJ, significantly affecting patients' quality of life. Although metabolic homeostasis in chondrocytes is crucial for cartilage health, the mechanisms underlying metabolic dysregulation in TMJOA remain poorly characterized. This study aimed to investigate the metabolic imbalance in TMJOA cartilage and explore novel therapeutic strategies targeting metabolic reprogramming. RNA sequencing revealed a significant imbalance between glycolysis and oxidative phosphorylation (OXPHOS) in TMJOA cartilage, with a marked shift toward glycolysis, which is associated with inflammation and cartilage degradation. To counteract this imbalance, Laccase domain-containing 1 (Lacc1), a metabolic regulator involved in both inflammation and metabolic homeostasis, was selected for investigation, as its role in chondrocytes had not been explored. We engineered macrophage-derived extracellular vesicles (EVs) to overexpress Lacc1 (OE-EVs), aiming to restore metabolic balance and modulate inflammation in chondrocytes. In vitro, OE-EVs significantly reduced IL-1β-induced inflammation, inhibited glycolysis by decreasing key glycolytic enzymes, improved mitochondrial function by decreasing mitochondrial superoxide levels, and the restoration of normal mitochondrial structure. In vivo, micro-computed tomography (Micro-CT) and histological analyses demonstrated that OE-EVs effectively alleviated inflammation and promoted cartilage repair, as indicated by a 1.55-fold increase in toluidine blue-stained cartilage area compared to the TMJOA group, reflecting improved cartilage matrix integrity and proteoglycan retention. These findings highlight the therapeutic potential of Lacc1-engineered EVs to target mitochondrial metabolism, reestablish metabolic homeostasis, and reduce inflammation in TMJOA, offering a novel and promising strategy for improving clinical outcomes in TMJOA patients.

*Correspondence:
Jian Xie
xjboom@163.com
Jiansheng Su
sjs@tongji.edu.cn

Full list of author information is available at the end of the article

Graphical abstract

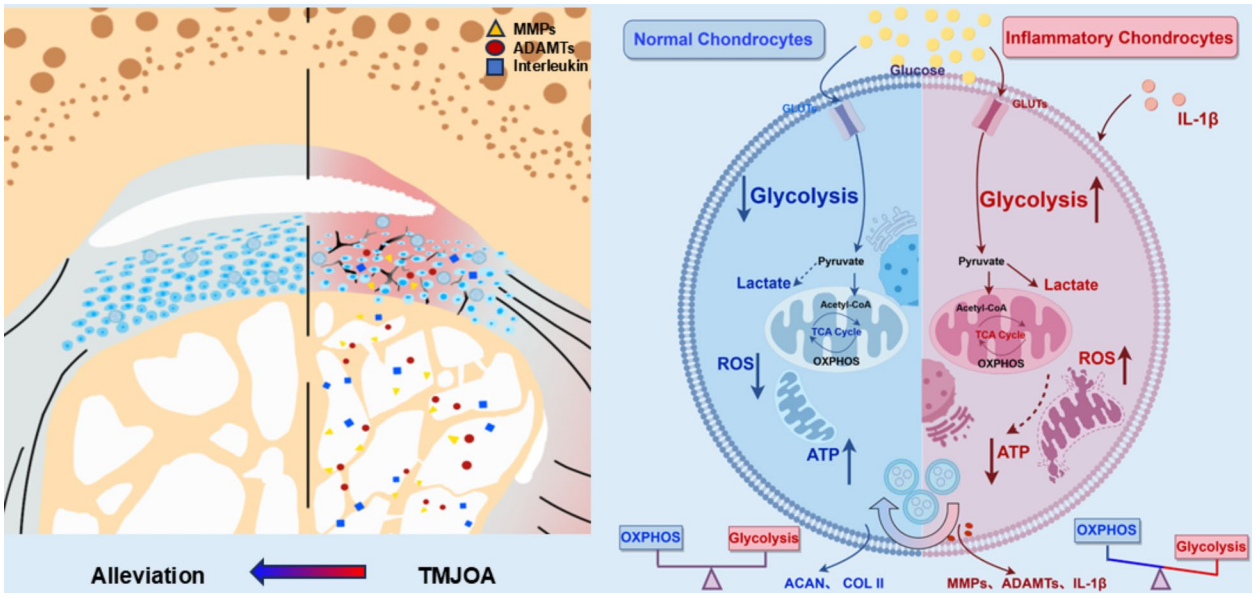

Keywords Temporomandibular joint osteoarthritis (TMJOA), Chondrocytes, Mitochondrial metabolism, Engineered extracellular vesicles, Laccase domain-containing 1 (Lacc1)

Introduction

The temporomandibular joint (TMJ) is one of the most complex joints in the human body, facilitating intricate movements including hinge and gliding activity. Temporomandibular joint osteoarthritis (TMJOA) is a chronic degenerative disease characterized by progressive cartilage degeneration, synovial inflammation, and orofacial pain, all of which severely impair patient quality of life [1–3]. Despite the availability of various pharmacological and physical treatment options, these therapies often fail to effectively halt or reverse the progression of TMJOA, highlighting the urgent need for more efficacious strategies that address the underlying pathophysiology of the disease [1, 4, 5].

Metabolic dysregulation within chondrocytes has recently emerged as a key driver of TMJOA progression [6, 7]. Chondrocytes primarily rely on glycolysis to meet their energy demands due to the hypoxic nature of cartilage [8, 9]. However, oxidative phosphorylation (OXPHOS) still plays a critical role in regulating chondrocyte homeostasis, contributing to ATP production, anabolic processes, and redox balance. In TMJOA, this metabolic balance is disrupted, leading to a pathological shift toward glycolysis at the expense of OXPHOS [10]. While glycolysis is necessary for chondrocyte survival in hypoxic conditions, excessive glycolytic activity is associated with inflammation and cartilage degradation. Pro-inflammatory cytokines, such as interleukin-1β (IL-1β), exacerbate this metabolic shift by further enhancing glycolysis, thereby amplifying the inflammatory response and accelerating disease progression [11]. Given these insights, restoring the balance between glycolysis and OXPHOS represents a promising strategy for mitigating TMJOA-associated metabolic and inflammatory dysregulation. Mitochondria serve as center for ATP generation and apoptosis regulation, making them pivotal in maintaining chondrocyte viability under inflammatory conditions. Mitochondrial dysfunction in the context of TMJOA leads to both chondrocyte death and enhanced inflammation, making it a crucial target for therapeutic intervention [12].

Recent studies have demonstrated that metabolic reprogramming not only influences chondrocyte survival and function but also intersects with inflammatory pathways, creating a vicious cycle that perpetuates cartilage degradation. In particular, the crosstalk between inflamed macrophages and metabolically dysregulated chondrocytes appears to exacerbate joint inflammation and tissue destruction [13]. Macrophages, which play a central role in inflammation, secrete pro-inflammatory cytokines (such as IL-1β and TNF-α) that disrupt chondrocyte metabolic pathways and further amplify joint inflammation and cartilage damage. Conversely, metabolically dysregulated chondrocytes can promote macrophage polarization toward a pro-inflammatory phenotype, creating a vicious cycle that accelerates

disease progression [14, 15]. This underscores the importance of macrophage–chondrocyte crosstalk in TMJOA pathogenesis and therapeutic strategies.

Therefore, extracellular vesicles (EVs) derived from macrophages provide a promising therapeutic tool to modulate both metabolic and immune responses in TMJOA. These EVs are capable of carrying bioactive molecules that modulate immune responses and metabolic reprogramming, making them ideal tools for treating TMJOA by restoring cellular balance and suppressing inflammation. Inflammatory macrophage-derived EVs promoted the expression of catabolic factors in chondrocytes and induce pyroptosis, contributing to cartilage degradation [16]. EVs derived from anti-inflammatory M2 macrophages can reduce inflammation and support cartilage repair in murine models of rheumatoid arthritis [17]. However, given the limitations of natural EV therapies, there is growing interest in engineered EVs, which enhance both the yield and therapeutic content by modifying the donor cells [18–20].

Given the emerging role of engineered EVs in modulating metabolic and inflammatory pathways, we sought to enhance their therapeutic potential by incorporating Lacc1, a metabolic regulator known to influence both glycolytic pathways and inflammatory responses in immune cells like macrophages [21, 22]. Lacc1-deficient mice exhibited elevated proinflammatory cytokines and exacerbated arthritis [23, 24]. While the role of Lacc1 in chondrocyte metabolism remains poorly understood, its ability to regulate key metabolic and immune pathways makes it an attractive target for therapeutic intervention in TMJOA. Elucidating the role of Lacc1 in this context may offer new therapeutic avenues for TMJOA. We hypothesize that Lacc1, when overexpressed in macrophage-derived EVs, could be delivered to chondrocytes to help restore metabolic balance, reduce inflammation, and promote cartilage repair. As natural mediators of intercellular communication, EVs offer a novel cell-free therapeutic strategy, capable of targeting specific cells within the joint and modulating their functions without the risks associated with direct cell therapies [19].

In this study, we first performed RNA sequencing to identify key metabolic imbalances in TMJOA chondrocytes, confirming the crucial roles of glycolysis and inflammatory signaling pathways in disease progression. We then developed and characterized Lacc1-overexpressing EVs (OE-EVs) and evaluated their therapeutic effects on TMJOA using both in vitro and in vivo models (Fig. 1). Our findings highlight the potential of OE-EVs to modulate chondrocyte metabolism, reduce inflammation, and ultimately promote cartilage regeneration. By investigating the metabolic and inflammatory crosstalk mediated by OE-EVs in TMJOA, our work provides new insights into the pathomechanisms of TMJ degeneration and offers a promising therapeutic approach for TMJOA through metabolic reprogramming and immune modulation.

Materials and methods

Materials and reagents

Dulbecco's modified Eagle's medium (DMEM), α-modified Eagle's medium (α-MEM), phosphate-buffered saline (PBS), Penicillin-Streptomycin solution and Trypsin solution were purchased from Hyclone Inc. (USA). Fetal bovine serum (FBS) was purchased from Oricell Biosciences (China). siLacc1 was conducted by RiboBio (China). The overexpression Lacc1 (OE-Lacc1) plasmid was conducted by GeneChem Co. Ltd (China). Trizol reagent and PrimeScript RT reagent Kit was purchased from Takara Inc. (Japan), and Hieff qPCR SYBR Green Master Mix was purchased from Yeasen Biotechnology Co., Ltd. (China). RIPA buffer and BCA protein Assay were purchased from Beyotime Biotechnology (China). The primary antibody of Lacc1 (sc-376231) was purchased from Santa Cruz biotechnology Inc. (USA). The primary antibodies of IL-6 (DF6087), Collagen II (AF0135), SOX9 (AF6330), JAK2 (AF6022), phospho-JAK2 (AF3024), STAT3 (AF6294), and phospho-STAT3 (AF3293) were purchased from Affinity BioScience LTD. (China). Primary antibodies of IL-1β (26048-1-AP), MMP3 (17873-1-AP), MMP9 (30592-1-AP), MMP13 (18165-1-AP), aggrecan (13880-1-AP), HK1 (15656-1-AP), HK2 (66974-1-Ig), LDHA (66287-1-Ig), PKM2 (15822-1-AP), Tubulin-β (10094-1-AP) and β-Actin (66009-1-Ig) were purchased from Proteintech Inc. (China). Primary antibody for Hif-1α (bs-0737R) was purchased from Bioss Inc. (China).

Cell culture

RAW 264.7 macrophages RAW 264.7 macrophages were purchased from ATCC and maintained in DMEM supplemented with 10% FBS and 1% penicillin-streptomycin at 37 °C in a humidified incubator with 5% CO_2.

Chondrocytes Primary chondrocytes were isolated from TMJ condylar cartilage of 3-week-old female C57BL/6 mice. After washing the cartilage fragments three times with PBS, they were digested with 0.25% (w/v) collagenase I and II (Sigma-Aldrich, USA) at 37 °C for 30 min. The digested tissue was centrifuged, and the resulting cells were filtered through a 40-μm cell strainer (Biosharp, China). Chondrocytes were then cultured in α-MEM with 15% FBS and 1% penicillin-streptomycin in a 5% CO_2 atmosphere at 37 °C. Cells were passaged at 75–85% confluence, with only passages 2 and 3 used for subsequent experiments.

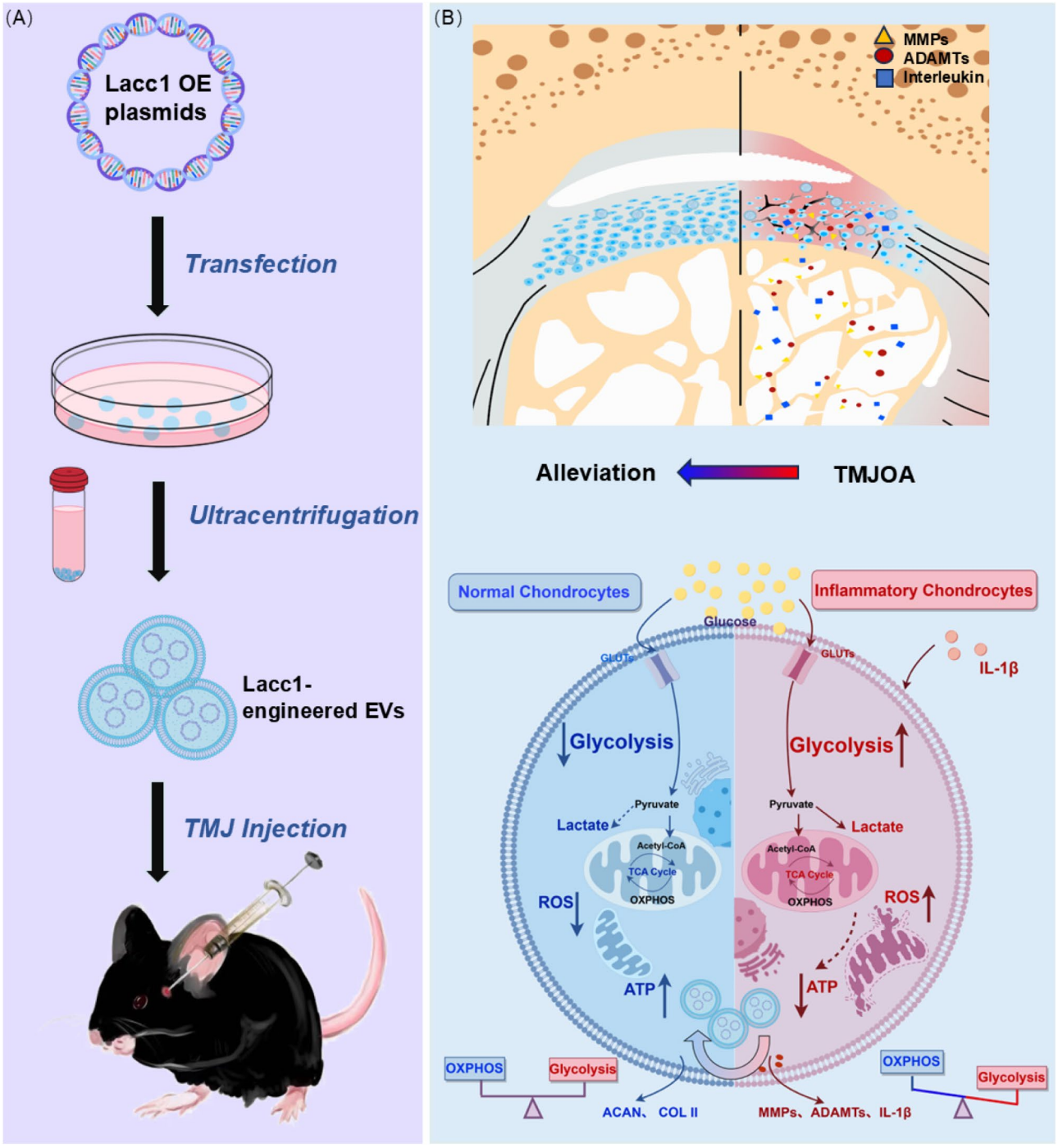

Fig. 1 The application of Lacc1-engineered EVs in TMJOA chondrocytes. (**A**) The construction of Lacc1-engineered EVs. (**B**) Lacc1-engineered EVs alleviated TMJOA inflammation via modulating mitochondrial metabolism in chondrocytes. (By Figdraw.)

Transfection of Lacc1 SiRNA and overexpressed Lacc1 plasmid

RAW 264.7 macrophages were treated with siLacc1 and OE-Lacc1 to investigate the role of Lacc1 in macrophage inflammation and glycolysis.

siLacc1

RAW 264.7 cells were transfected with siLacc1 using Lipofectamine 3000 (Invitrogen, USA) according to the manufacturer's instructions, followed by treating with 100 ng/mL lipopolysaccharide (LPS; Sigma, USA) for 24 h. qRT-PCR was conducted to assess the expression

levels of Lacc1, TNF-α, IL-1β, IL-6, iNOS, Arg-1, and MMP13, along with the expression of glycolysis-related genes (Acod1, PKM2, PFKp, and HK1). Additionally, ATP levels were measured as well.

OE-Lacc1

RAW 264.7 cells were transfected with Lacc1 overexpression plasmids using PEI transfection reagent (Transgen, China) according to the manufacturer's protocol, followed by treating with 100 ng/mL LPS for 24 h. qRT-PCR was then performed to assess the expression of Lacc1, IL-1β, IL-6 and MMP13. Western blot analysis was conducted to determine the expression levels of Lacc1, IL-6, iNOS, and MMP9.

Preparation and characterization of Lacc1-engineered EVs (OE-EVs)

Preparation

RAW 264.7 macrophages were transfected with overexpression (OE) Lacc1 or negative control (NC) plasmids using PEI transfection reagent following the manufacturer's protocol. After 12 h, the transfection medium was replaced with α-MEM containing 10% exosome-depleted FBS. After 3 days, OE-EVs and NC-EVs were isolated by ultracentrifugation, respectively. Briefly, the cell culture supernatant was firstly centrifuged at 300 g for 10 min at 4 °C. The supernatant was then transferred to a fresh tube and centrifuged at 10,000 g for 10 min at 4 °C. Next, the supernatant was placed in an ultracentrifuge tube and centrifuged at 100,000 g for 90 min at 4 °C. The supernatant was discarded, and the precipitate was resuspended in PBS and centrifuged again at 100,000 g for 90 min at 4 °C. The final precipitate was resuspended in 200μL of PBS, filtered through a 0.22-μm filter, and stored at -80 °C until use.

Characterization

Transmission electron microscopy (TEM; FEI, USA) was employed to examine the morphology of extracellular vesicles (EVs). Both OE-EVs and NC-EVs were fixed overnight at 4 °C in 2.5% glutaraldehyde. A volume of 10μL liquid was placed on a copper grid for 5 min, followed by staining with saturated uranyl acetate for 1 min. The grid was then rinsed twice with ddH_2O and air-dried prior to observation. Nanoparticle Tracking Analysis (NTA; Malvern, UK) was then conducted to assess the concentration and size distribution of EVs. Additionally, Western blot analysis was performed to identify key proteins associated with EVs, including CD63, CD81, and TSG101, along with Calnexin as a negative control, and to quantify Lacc1 levels within the EVs.

The uptake of EVs in chondrocytes

NC-EVs and OE-EVs were labeled with PKH 26 (MCE, USA) according to the manufacturer's instructions. The EVs were then resuspended in PBS and centrifuged at 100,000 g for 90 min at 4 °C to remove excess dye. The labeled EVs were incubated with chondrocytes for 12 h. After incubation, the cells were fixed and stained with phalloidin and Hoechst. Finally, EV uptake by chondrocytes was visualized using a laser confocal microscope (Leica, Germany).

Biocompatibility

To evaluate the potential cytotoxic impacts of OE-EVs/NC-EVs on chondrocytes, the cell count kit-8 (CCK-8; Dojindo, Japan) was performed. Chondrocytes were incubated with different concentrations (0, 5, 15, 25 and 35 μg/mL) of OE-EVs/NC-EVs for durations of 24, 48, or 72 h, followed by the addition of CCK-8 solution. After 1 h, the OD at 450 nm was measured with microplate reader. Cell viability of chondrocytes was determined by live-dead assay kits (Dojindo, Japan), following manufacturer's protocol. Fluorescence microscopy was used to take photos of live and dead cells.

In vitro inflammation model of chondrocytes

In vitro inflammation induction

Chondrocytes were seeded in 12-well plates at a density of 4 × 10^4 cells per well. After 24 h, the original medium was replaced with fresh culture medium containing 10 ng/mL interleukin-1β (IL-1β; PeproTech, USA) for an additional 24 h. Subsequently, the IL-1β-induced chondrocytes were treated with OE-EVs (15 μg/mL) or NC-EVs (15 μg/mL) for 24 h.

Quantitative Real-Time polymerase chain reaction (qRT-PCR)

Total RNA was isolated using Trizol reagent and reverse transcribed into cDNA using the PrimeScript RT Reagent Kit, following the manufacturer's instruments. qRT-PCR was performed using the Hieff qPCR SYBR Green Master Mix on a QuantStudio 5 Real-Time PCR System (Thermo Fisher Scientific, USA). Relative expression level of target genes was calculated using the $2^{-\Delta\Delta Ct}$ method. Primers sequences are shown in Tables S1.

Western blot analysis

Total proteins were extracted from the collected cells using RIPA buffer, and protein concentration was determined via a BCA protein Assay. Equal amounts of protein were separated by Omni-PAGE (Epizyme Biotech, China) and transferred to nitrocellulose membranes. The membranes were blocked with 5% bovine serum albumin (BSA) for 1 h at room temperature and then incubated overnight at 4℃ with the primary antibodies. Following this, the membranes were treated with secondary antibodies for 1 h at room temperature. Protein bands were visualized by a chemiluminescence detection system

(Cytiva, UK), with Tubulin/β-Actin serving as the loading control.

Immunofluorescence (IF) staining

Samples were fixed in 4% paraformaldehyde for 15 min at room temperature, washed three times with PBS and permeabilized with 0.5% Triton X-100. After blocking with 3% BSA, the samples were incubated with primary antibody of aggrecan and MMP13 overnight at 4℃. Following three washes with PBS, the cells were incubated with a fluorescent secondary antibody for 1 h at room temperature in the dark. After an additional three washes, the plates were sealed with DAPI anti-fluorescence quenching solution.

ELISA analysis

The culture supernatant was collected to quantify the concentration of IL-1β using commercial ELISA kits, following the manufacturer's instructions.

Mitochondrial function detection of chondrocytes

Mitochondria membrane potential assay

Mitochondria membrane potential (ΔΨ) was assessed using JC-1 staining. Briefly, cells were incubated with 2 μM JC-1 for 20 min at 37 °C. After three washes with PBS, fluorescence images were captured using a fluorescent inverted microscope (Nikon, Japan).

Intracellular and mitochondrial ROS assay

The generation of intracellular ROS was measured using a ROS Assay Kit (Beyotime Biotechnology, China). Chondrocytes treated with IL-1β were exposed to OE-EVs or NC-EVs for 24 h, followed by incubation with 10μM DCFH-DA for 20 min at 37℃. After washing three times with PBS, images were obtained using fluorescence microscopy.

For mitochondrial superoxide detection, the chondrocytes were incubated with 100 nM MitoTracker Green FM (MCE, USA) and 5 μM MitoSox Red (Invitrogen, USA) for 15 min at 37℃. After being washed with PBS for three times, a laser confocal microscope (Leica, Germany) was applied for recording the photographs.

Cell ATP level assay

Chondrocytes were seeded in 12-well plates at a density of 4×10^4 cells per well. The ATP levels in various groups were determined by using the Enhanced ATP Assay Kit (Beyotime Biotechnology, China) and analyzed based on the luminescence intensity.

Cell lactic acid production assay

Chondrocytes were seeded in 12-well plates at a density of 4×10^4 cells per well and incubated with IL-1β (10 ng/mL) for 24 h. Subsequently, the chondrocytes were treated with OE-EVs or NC-EVs for another 24 h. Then the supernatants were collected, and lactic acid concentration was measured using the L-Lactic Acid Colorimetric Assay Kit (Elabscience, China), according to the manufacturer's protocol.

Observation of mitochondrial morphology

Chondrocytes treated with IL-1β were incubated with either OE-EVs or NC-EVs for 24 h, followed by harvesting via centrifugation and fixation with 2.5% glutaraldehyde solution at 4 °C overnight. The chondrocyte pellets were then post-fixed in osmium tetroxide, dehydrated in an ethanol gradient, and infiltrated with epoxy resin for embedding and sectioning. Transmission electron microscopy (TEM) was used to examine mitochondrial quantity, morphology, and ultrastructural changes in chondrocytes.

RNA sequence analysis

To explore differentially expressed genes (DEGs) between TMJOA and normal condyles, samples from TMJOA and normal condyles were collected and preserved in Trizol reagent. Additionally, to elucidate the potential mechanisms underlying the modulation of chondrocytes inflammation by OE-EVs, various groups of chondrocytes underwent the specified treatments and were subsequently lysed using Trizol. The tissue samples from condyles and chondrocytes lysates were then submitted to Novogene Corporation Inc. (China) for transcriptome sequencing.

Following the identification of DEGs, differential gene clustering was performed, and volcano map was generated to visualize the expression changes. The resulting alterations in signaling pathways were analyzed using Gene Set Enrichment Analysis (GSEA), Kyoto Encyclopedia of Genes and Genomes (KEGG) and Gene Ontology (GO) enrichment analyses.

Animal experiments

A total of 24 C57BL/6 mice (8-week-old, male) were utilized in this study. The mice were randomly allocated to four groups: Con ($n = 6$), OA + PBS ($n = 6$), OA + NC-EVs ($n = 6$), OA + OE-EVs ($n = 6$). All animal experimental protocols were approved by Animal Welfare Committee of Stomatological Hospital of Tongji University (Approved No. 2024-DW-19).

For the induction of TMJOA model, unilateral discectomy of the left TMJ disc was performed in age-matched male mice, following a previously established method. Two weeks post-induction, the mice received intra-articular injections twice weekly for four weeks, at a volume of: 100 μg of NC-EVs in 25 μL of PBS for the TMJOA + NC-EVs group, 100 μg of OE-EVs in 25 μL of PBS for the TMJOA + OE-EVs group, 25 μL PBS for the

TMJOA group. Meanwhile, the age-matched naive control group remained untreated.

In vivo imaging of PKH26-Labeled EVs

To evaluate the in vivo distribution and metabolism of EVs, PKH26-labeled EVs (100 μg) were injected into the TMJ cavity of mice. The fluorescence signal was monitored at 0 h, 24 h, and 72 h post-injection using an in vivo imaging system (Berthold, Germany). At each time point, mice were anesthetized and positioned in the imaging chamber for whole-body and TMJ-specific imaging. The fluorescence intensity and distribution were analyzed using Indigo imaging software to assess EV retention and clearance at different time points.

Microcomputed tomography (micro-CT) analysis

Following four weeks of treatment, the animals were euthanized, and the TMJ condyles were isolated and fixed in 4% paraformaldehyde for 48 h. The samples were scanned using a Scanco mCT 50 (Scanco Medical, Switzerland) at a scan resolution of 10-μm and a voltage of 70 kVp. The sagittal and top views of the condyle were reconstructed. CTAn software (Bruker microCT, Kontich, Belgium) were employed to evaluate the structural properties of bones, including the percentage of bone volume over total volume (BV/TV, %), trabecular thickness (Tb·Th, mm), trabecular separation (Tb.Sp, mm), and trabecular number (Tb·N, 1/mm).

Histological analyses

TMJ specimens were decalcified in 10% EDTA for 4 weeks prior to histological processing. After dehydration, the specimens were embedded in paraffin and sectioned at 5 μm using a microtome. The sections were stained with hematoxylin and eosin (H&E) (Beyotime Biotechnology, China), Toluidine blue (T.B.) (Solarbio, China) and Safranin O/Fast Green (Solarbio, China) according to the manufacturer's protocols. Osteoarthritis Research Society International (OARSI) scoring system was used to evaluate the grading of OA progress and cartilage degeneration in each group.

Immunohistochemistry (IHC) and Immunofluorescence (IF) analyses

IHC staining was performed using an IHC kit (Maxin, China). Deparaffinized sections were dehydrated with xylene and ethanol, followed by incubation in antigen retrieval solution for 1 h at 37℃. Subsequently, the samples were treated with endogenous peroxidase blocking buffer and a non-specific staining blocking buffer, adhering to the manufacturer's instructions. Primary antibodies against Collagen II (COL II) and IL-1β were incubated at 4 ℃ overnight. After washing three times with PBS, biotinylated secondary antibodies were applied for 10 min at room temperature, followed by additional washes with PBS. Subsequently, the samples were treated with streptavidin-HRP and incubated for 10 min at room temperature. After three PBS washes, DAB chromogenic droplets were added in the dark for 3 min followed by rinsing with tap water for 5 min. Subsequently, the samples were then counterstained with hematoxylin, dehydrated with ethanol, cleared with xylene, and sealed with neutral resin before imaging.

For IF staining, sections were incubated with primary antibodies against aggrecan, MMP3 and MMP13 at 4℃ overnight. After being washed with PBS for 3 times, the sections were incubated with fluorescent secondary antibody for 1 h at room temperature in the dark. DAPI was used for the nuclear staining. Images were captured using a laser confocal microscope (Nikon, Japan).

Statistical analysis

Experimental data were analyzed using paired t-tests and one-way analysis of variance (ANOVA) via GraphPad Prism 8.0 software. All experiments were conducted with at least three independent biological replicates ($n = 3$), unless otherwise specified. Statistical significance was designated as follows: ns (not significant), $^{*}p < 0.05$, $^{**}p < 0.01$, and $^{***}p < 0.001$, as illustrated in the figures.

Results and discussion

Dysregulation of Glycolysis and OXPHOS homeostasis in TMJOA cartilage

To explore gene expression alterations in the condyles of TMJOA mice, condyle tissues from both normal and TMJOA mice were collected for transcriptomic analysis. As Fig. 2A depicted, sequencing results demonstrated a significant upregulation of glycolysis-related genes, including HK3 (Hexokinase 3) and Pklr (Pyruvate kinase). In contrast, key genes related to oxidative phosphorylation (OXPHOS) and TCA cycle, including Cs (Citrate synthase), Mdh2 (Malate dehydrogenase), and Sdhc (Succinate dehydrogenase), were markedly downregulation.

Hexokinase (HK), including HK1, HK2, HK3, HK4, and HKDC1, play critical roles in glucose metabolism, catalyzing the initial step of glucose utilization [25]. The upregulation of HKs suggests enhanced glycolytic activity. Citrate synthase (Cs) initiates the tricarboxylic acid (TCA) cycle by catalyzing the condensation of oxaloacetate and acetyl-CoA [26]. Moreover, Mdh2, a crucial enzyme in the TCA cycle, contributes to energy production and stabilizes hypoxia-inducible factor 1 alpha (HIF-1α), linking metabolism to cellular responses to hypoxia [27]. Sdhc, serves as a pivotal enzyme bridging the TCA cycle and OXPHOS pathway, its downregulation further indicates disrupted energy metabolism in TMJOA cartilage [28].

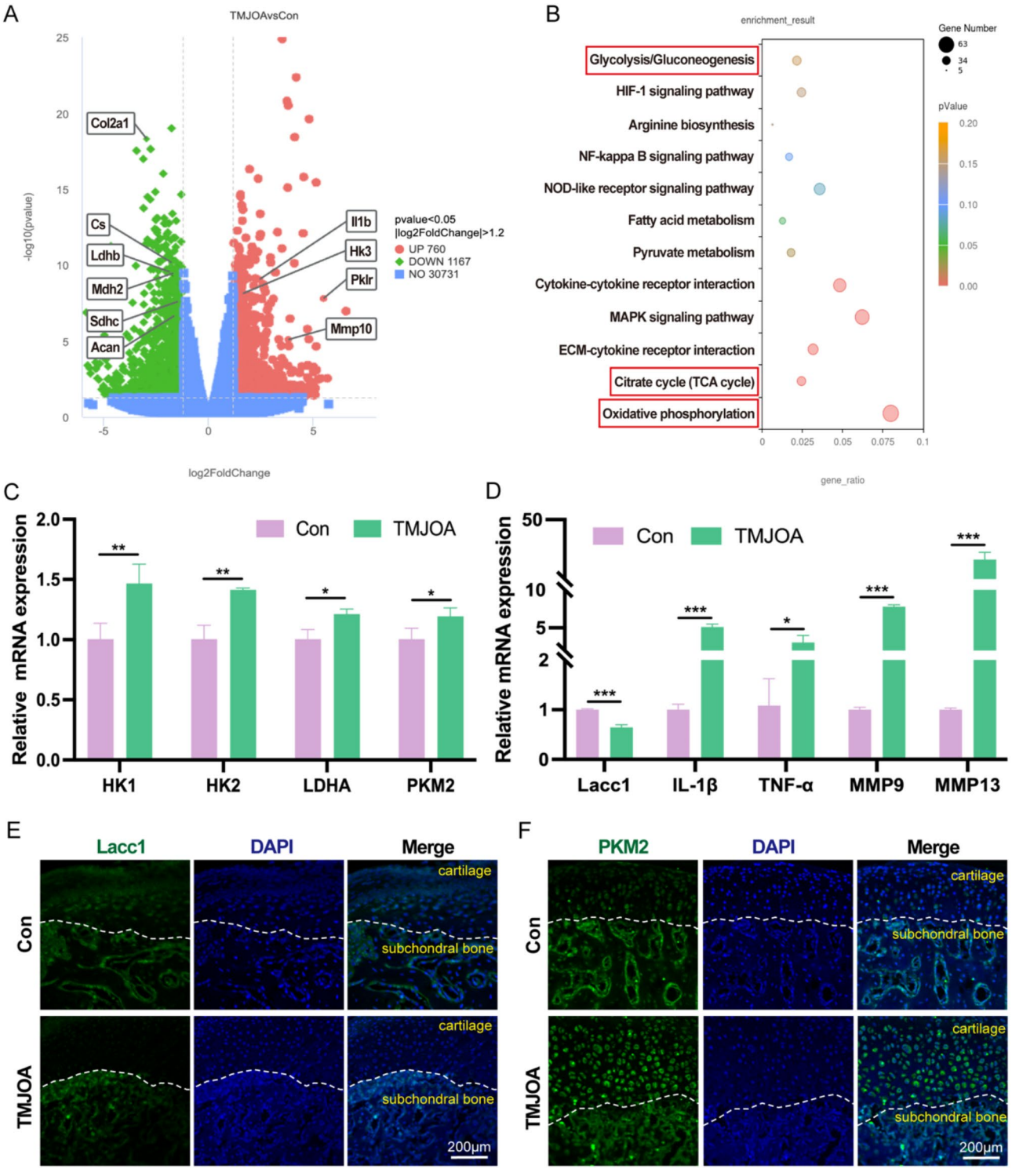

Fig. 2 Metabolic Dysregulation in TMJOA Cartilage. (**A**) Volcano plot of differentially expressed genes in TMJOA cartilage. (**B**) KEGG pathway enrichment analysis of metabolism-related signaling pathways. (**C**&**D**) qRT-PCR analysis of glycolytic enzymes, Lacc1, and inflammatory cytokines in TMJOA cartilage. (**E**&**F**) Immunofluorescence staining of Lacc1 and PKM2 in TMJOA cartilage. ($n = 3$, *$p < 0.05$, **$p < 0.01$, and ***$p < 0.001$)

Additionally, the expression of structural cartilage matrix genes, Col2a1 (collagen II) and acan (aggrecan) was significantly decreased, while IL-1β and matrix metalloproteinases 10 (MMP10) levels were markedly elevated in the TMJOA condylar cartilage. Kyoto Encyclopedia of Genes and Genomes (KEGG) analysis indicated that differentially expressed genes were primarily enriched in pathways related to "Oxidative phosphorylation", "Citrate cycle (TCA cycle)", "Glycolysis/Gluconeogenesis" and others (Fig. 2B). These alterations indicate a metabolic shift towards enhanced glycolytic activity in TMJOA condylar cartilage, contrasting with a decrease in TCA cycle and OXPHOS functionality compared to normal cartilage.

To validate the expression of key metabolic enzymes, qRT-PCR was performed, revealing significant upregulation of glycolysis-associated genes, including HK1, HK2, Lactate dehydrogenase (LDHA), and Pyruvate kinase (PKM2) in OA cartilage (Fig. 2C). The expression levels of Lacc1 and pro-inflammatory cytokines were also assessed. As shown in Fig. 2D, pro-inflammatory markers such as IL-1β, matrix metalloproteinases (including MMP9, MMP13) and tumor necrosis factor-α (TNF-α) were markedly elevated in OA cartilage. Previous researches indicated that IL-1β played a crucial role in OA by promoting the upregulation of matrix metalloproteinases (MMPs), which contributed to the irreversible breakdown of extracellular matrix (ECM) and progression of OA [1, 29]. In contrast, both qRT-PCR results (Fig. 2D) and immunofluorescence staining for Lacc1 (Fig. 2E) demonstrated a significant downregulation of Lacc1 in TMJOA cartilage, suggesting its potential anti-inflammatory role and its relationship with glycolysis in chondrocytes.

Furthermore, Fig. 2F illustrated a pronounced expression of PKM2, a key glycolytic enzyme, in TMJOA group. Previous studies have highlighted that the metabolism reprogramming played a vital role in knee OA, with inflamed chondrocytes shifting their metabolism towards glycolysis, resulting in LDHA accumulation and increased reactive oxygen species (ROS) generation [29]. Enzymes such like pyruvate kinase (PKM), lactate dehydrogenase (LDHA) and hexokinase (HK) are integral to regulating glucose metabolism, and IL-1β induction significantly elevated the expression of those genes in chondrocytes [29, 30]. Collectively, our findings indicate an imbalance between glycolysis and OXPHOS in TMJOA cartilage, with Lacc1 potentially acting as a metabolic link in the pathogenesis of TMJOA.

Validation of the function of Lacc1 in RAW264.7 macrophages

To elucidate the role of Lacc1 in RAW264.7 macrophages, we performed both siRNA-mediated knockdown and Lacc1 overexpression experiments. Initially, qRT-PCR was employed to identify the most effective siRNA for Lacc1 knockdown (Fig. S1A). The optimal siRNA was selected for subsequent analysis to evaluate its effect on macrophage polarization upon LPS treatment. As Fig. S1B depicted, siLacc1 treatment increased the expression of pro-inflammatory cytokines including TNF-α, IL-1β and inducible nitric oxide synthase (iNOS), while significantly reducing the expression level of Arginase-1 (Arg-1), a marker associated with anti-inflammatory M2 macrophages [31, 32], suggesting a shift toward a pro-inflammatory phenotype in siLacc1-treated macrophages. Subsequently, the expression of glycolysis related genes were also assessed by qRT-PCR. Fig. S1C illustrated that siLacc1 markedly elevated the expression of aconitate decarboxylase 1 (Acod1), PKM2, phosphofructokinase (PFKp) and HK1, which served important roles in the process of glycolysis [25, 33]. Furthermore, ATP level measured in Fig. S1D indicated that siLacc1 led to lower ATP production, regardless of LPS stimulation, compared to the siNC group.

Subsequently, Lacc1 overexpression plasmids were transfected into RAW264.7 macrophages to assess the effects of Lacc1 on inflammation and metabolism. The enhanced expression of Lacc1 in the transfected cells, compared to the negative control (NC) group, was confirmed through fluorescence microscopy, quantitative real-time PCR (qRT-PCR), and western blot analyses (Fig. S2A-S2C). Then qRT-PCR and Western blot analysis was conducted to detect the effects of Lacc1 overexpression on inflammatory responses of macrophages. As presented in Fig. S2D & S2E, Lacc1 expression was significantly elevated in the overexpression (OE) group. In contrast, the levels of IL-1β, IL-6, iNOS, MMP9, and MMP13 were substantially decreased in the OE group compared to the NC group.

In summary, our data indicate that Lacc1 plays a pivotal role in regulating both inflammation and glycolysis in RAW264.7 macrophages. Thus, RAW264.7 macrophages engineered to overexpress Lacc1 could represent a promising source for the development of extracellular vesicles aimed at regulating metabolism and suppressing inflammation.

Lacc1-Engineered EVs (OE-EVs) alleviated IL-1β induced inflammation in chondrocytes

Construction and characterization of OE-EVs

In this study, RAW264.7 macrophages were transfected with a plasmid for Lacc1 overexpression. Following transfection, Lacc1-engineered vesicles (OE-EVs) were isolated from the treated RAW264.7 macrophages using ultracentrifugation, while the vesicles from NC plasmid-treated cells were designated as NC-EVs.

The morphology of OE-EVs and NC-EVs was evaluated using transmission electron microscopy (TEM). As illustrated in Fig. 3A, both OE-EVs and NC-EVs exhibited typical exosomal morphology, characterized by a saucer-like or hemispherical shape with concave surfaces. Nanoparticle tracking analysis (NTA) (Fig. 3A) revealed average sizes of 126.1 nm for OE-EVs and 128.3 nm for NC-EVs, aligning with the expected EV size range (30–200 nm). The concentrations of OE-EVs and NC-EVs were quantified as 1.35×10^{10} particles/mL and 1.6×10^{10} particles/mL, respectively. The protein content of OE-EVs was determined to be 0.82 mg/mL, while NC-EVs had 0.66 mg/mL. Western blot analysis in Fig. 3C confirmed the presence of exosomal markers CD63, CD81, and TSG101 in both OE-EVs and NC-EVs, while the negative marker Calnexin was not detected. Additionally, Lacc1 expression was significantly higher in OE-EVs group than that in the NC-EVs group.

The uptake efficiency of OE-EVs by chondrocytes was assessed by labeling the vesicles with PKH26 dye [34]. As illustrated in Fig. 3B, both OE-EVs and NC-EVs were effectively internalized by chondrocytes, primarily localized in the cytoplasm. PKH26 was selected for EV labeling due to its high membrane affinity, strong fluorescence stability, and extensive use in EV research. PKH26 has been widely utilized to track EV uptake and biodistribution in various disease models, including osteoarthritis and rheumatoid arthritis [35]. Compared to other dyes, PKH26 offers low photobleaching, ensuring long-term visibility of labeled EVs in both in vitro and in vivo settings, making it a reliable tool for tracking EV-mediated cellular interactions. To assess biocompatibility, chondrocytes were treated with various concentrations of OE-EVs and NC-EVs for 1, 3, and 5 days, followed by cell viability assessment using the CCK-8 assay. As shown in Fig. S3A, chondrocytes treated with 15 μg/mL OE-EVs demonstrated the highest viability across all time points. Consequently, 15 μg/mL OE-EVs and NC-EVs were utilized in subsequent experiments. To further assess the protective effects of EVs on chondrocytes in an inflammatory environment, calcein-AM/PI live/dead cell staining was performed. Fig. S3B revealed more dead cells in the IL-1β-treated group while fewer dead cells were observed in the Con, NC-EVs, and OE-EVs groups, suggesting that both OE-EVs and NC-EVs had favorable biocompatibility and protective effects. These results confirm that OE-EVs and NC-EVs have favorable biocompatibility and are efficiently endocytosed by chondrocytes.

OE-EVs alleviated IL-1β induced inflammation in chondrocytes in vitro

Diminishing inflammation and promoting cartilage matrix synthesis are crucial for the effective treatment of TMJ osteoarthritis. To evaluate the therapeutic effects of OE-EVs on IL-1β induced inflammatory chondrocytes, we assessed the expression of key markers involved in cartilage matrix formation and the inflammatory cytokines. As shown in Fig. 3D, qRT-PCR results indicated a significant reduction in the expression of collagen II, aggrecan, and Sox9, key markers for cartilage matrix synthesis in IL-1β group. However, treatment with OE-EVs resulted in a significant upregulation of these markers, indicating that OE-EVs promote cartilage matrix synthesis under inflammatory conditions. Moreover, the expression of inflammatory cytokines (including IL-1β and IL-6), and matrix metalloproteinase (including MMP9 and MMP13) was markedly elevated following IL-1β induction, whereas OE-EVs treatment effectively downregulated these cytokines.

Western blot analysis corroborated these findings. As illustrated in Fig. 3H, the levels of IL-1β, IL-6, MMP3, and MMP9 were significantly enhanced with IL-1β stimulation. However, the OE-EVs treatment effectively counteracted the pro-inflammatory effects of IL-1β. The expression of Sox9 showed an opposite trend, further supporting the potential of OE-EVs in promoting cartilage matrix synthesis and chondrocyte anabolic metabolism.

To further assess the impact of OE-EVs on inflammatory cytokine secretion, ELISA was conducted. Figure 3F demonstrated that OE-EVs reduced the excessive secretion of IL-1β, further confirming their anti-inflammatory properties. In addition, immunofluorescence staining for aggrecan (Fig. 3E) and MMP13 (Fig. 3G) in chondrocytes showed that IL-1β stimulation decreased aggrecan expression while increasing MMP13 expression. Conversely, OE-EVs treatment counteracted these effects, resulting in higher aggrecan levels and lower MMP13 expression.

To further investigate the mechanism by which OE-EVs modulate the inflammatory response, we examined their effect on macrophages. RT-PCR and Western blot analyses of LPS-stimulated macrophages treated with OE-EVs revealed a significant downregulation of pro-inflammatory markers, including TNF-α, MMP9, MMP13, IL-1β, and iNOS, while the expression of Arg1 was markedly increased (Fig. S4). These findings indicate that OE-EVs primarily function by suppressing M1 macrophage polarization, thereby mitigating the inflammatory phenotype.

In articular cartilage, the extracellular matrix (ECM) is primarily composed of aggrecan and type II collagen. Aggrecan plays a pivotal role in maintaining cartilage phenotype and promoting chondrocyte proliferation, while type II collagen, encoded by the gene COL2A1 and synthesized by chondrocytes, is a major structural collagen [36–38]. Sox9, a transcription factor crucial for chondrogenesis, is expressed from the multifunctional mesenchymal precursor stage to the cell differentiation

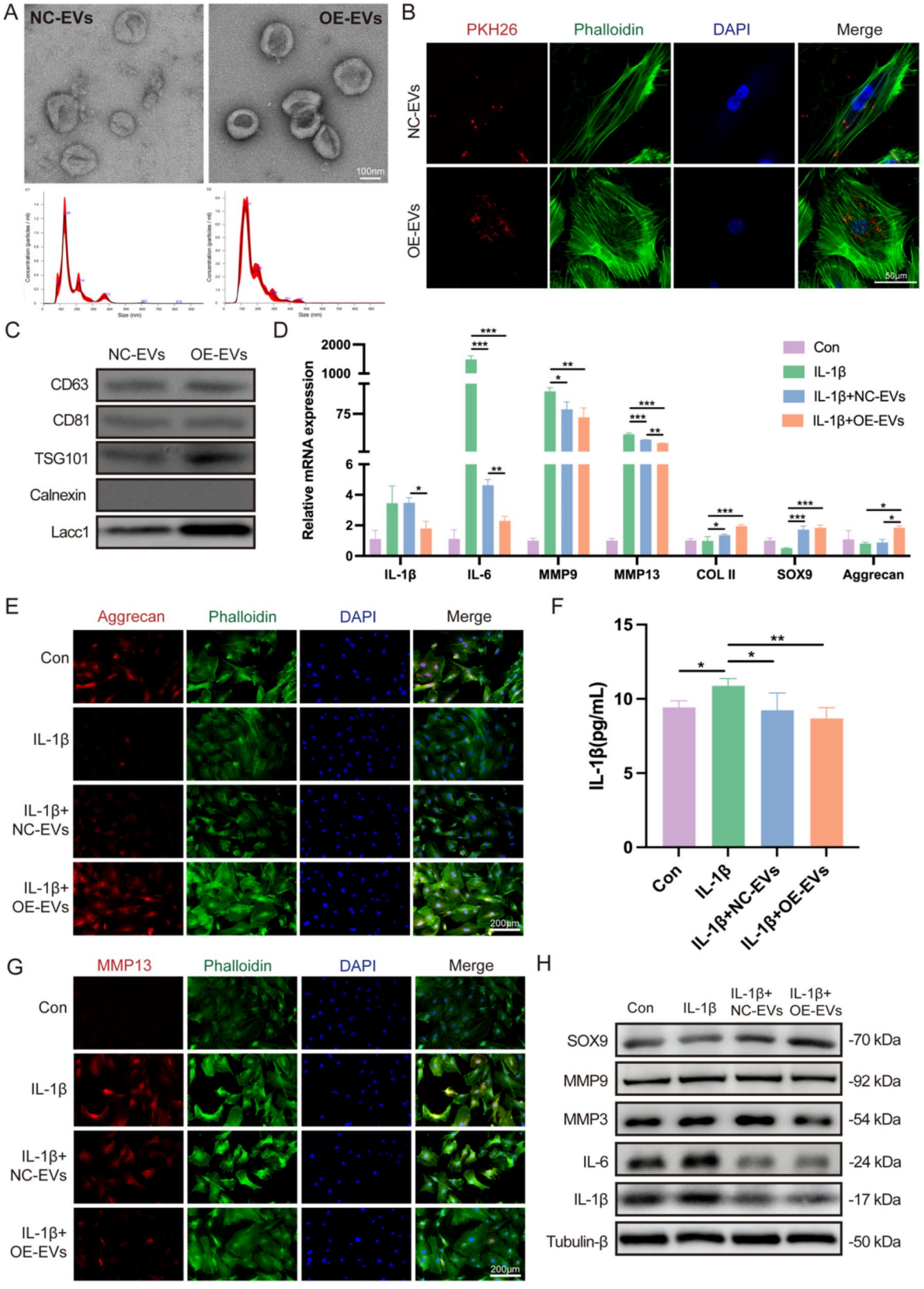

Fig. 3 OE-EVs attenuate IL-1β-induced inflammation in chondrocytes. (**A**) TEM and NTA characterization of NC-EVs and OE-EVs. (**B**) PKH26-labeled EVs internalized by chondrocytes. (**C**) Western blot analysis of exosomal markers and Lacc1 in NC-EVs and OE-EVs. (**D**) qRT-PCR of inflammatory and cartilage matrix markers. (**E**&**G**) Immunofluorescence staining of Aggrecan and MMP13. (**F**) IL-1β levels measured by ELISA. (**H**) Western blot of inflammation- and ECM-related markers. ($n = 3$, $^{*}p < 0.05$, $^{**}p < 0.01$, and $^{***}p < 0.001$)

stage, and its inactivation hindered the development of cartilage [39]. Therefore, these cartilage-specific genes are essential for sustaining chondrocyte function and programming anabolic metabolism.

However, in the inflammatory environment of OA, pro-inflammatory cytokines (such as IL-1β and IL-6) and matrix-degrading enzymes (such as MMP3, MMP9, MMP13, and ADAMTS5) promote inflammation and catabolic metabolism, leading to ECM degradation and impaired chondrocyte function. IL-1β is significantly increased in synovial fluid of TMJOA patients and mediates matrix degradation via inducing expression of matrix degradative enzymes such as MMP3, MMP9, MMP13 and ADAMTS5 [39, 40]. Besides, elevated by inflammation, excessive production of reactive metabolites, including reactive oxygen (ROS) and reactive nitrogen species (RNS), contribute to mitochondrial dysfunction, matrix degradation, and cell damage in OA [9]. These factors create a vicious cycle that exacerbates cartilage degeneration.

Previous studies have demonstrated that MSC-derived exosomes can ameliorate inflammation in TMJOA by reducing IL-1β and iNOS expression [40]. Moreover, engineered EVs have been reported to deliver functional molecules, such as miRNAs, to repair the immune microenvironment in OA joints, thereby alleviating OA progression [41]. Recent research highlights the crucial role of synovial macrophages in OA pathogenesis, as they secrete pro-inflammatory cytokines that interact with chondrocytes and exacerbate cartilage degradation [14]. Additionally, macrophage-derived EVs have been implicated in cartilage catabolism and synovial inflammation, further underscoring their contribution to OA progression [42]. In line with these findings, our results demonstrate that OE-EVs not only protect cartilage ECM homeostasis by enhancing matrix synthesis and inhibiting degradation but also mitigate chondrocyte inflammation in vitro. These findings strongly support the potential of OE-EVs as a novel metabolic and immunomodulatory therapy for OA, paving the way for future investigations into their role in regulating energy metabolism.

OE-EVs reprogrammed chondrocytes' energy metabolism by alleviating mitochondria dysfunction

Energy metabolism is a crucial mediator of cellular function and is often altered during disease states, particularly in response to inflammatory stimuli in chondrocytes. Previous studies have demonstrated the therapeutic effects of OE-EVs on chondrocytes in vitro. To further investigate the metabolic changes in IL-1β-induced inflammatory chondrocytes, gene and protein expression related to key enzymes involved glycolysis were analyzed by qRT-PCR and Western blotting. As shown in Fig. 4A and B, IL-1β treatment resulted in a significant increase in the expression of HK1, HK2, LDHA, PKM2 and hypoxia-inducible factor 1-alpha (Hif-1α), indicating enhanced glycolysis activity in OA chondrocytes. Notably, treatment with OE-EVs effectively counteracted these changes.

Mitochondria play a central role in ATP synthesis and cellular metabolism. Inflammation-induced mitochondrial dysfunction is characterized by impaired ATP production. To assess the impact of OE-EVs on mitochondria dysfunction induced by inflammation, we performed cell ATP assay. As illustrated in Fig. 4C, IL-1β significantly reduced ATP level in chondrocytes, while OE-EVs treatment effectively restored the ATP level.

Moreover, we measured the extracellular lactate levels in the supernatants of various groups. As depicted in Fig. 4D, lactate concentration was markedly elevated in the IL-1β group, whereas OE-EVs treatment led to a significant reduction. Additionally, mitochondrial dysfunction is characterized by an aberrant change in the mitochondrial membrane potential ($\Delta\Psi_m$). JC-1 staining (Fig. 4E) revealed that IL-1β-treated chondrocytes exhibited increased green fluorescence from JC-1 monomers (indicating ΔΨm loss), whereas OE-EVs treatment resulted in prominent red fluorescence from JC-1 aggregates, suggesting ΔΨm restoration.

Excessive ROS production contributes to oxidative stress and mitochondrial dysfunction, exacerbating cellular damage. DCFH-DA staining (Fig. S5) demonstrated a significant increase in intracellular ROS levels in the IL-1β group, which were effectively reduced by OE-EVs treatment. We also evaluated mitochondrial ROS levels using MitoSOX staining and examined mitochondrial morphology with MitoTracker Green staining. As shown in Fig. 4F, inflammatory chondrocytes exposed to IL-1β exhibited impaired mitochondrial morphology, including mitochondrial deformation, swelling. Conversely, OE-EVs treatment mitigated these detrimental effects. Mitochondrial ROS (mtROS) level significantly increased in IL-1β group, implying an escalation in mitochondrial oxidative stress damage, however, remarkably inhibited with OE-EVs treatment. As shown in Fig. 4G, the IL-1β group displayed severely damaged mitochondrial structures, such as reduced crista, disrupted membranes, and a swollen phenotype, compared to Control group. In contrast, chondrocytes treated with OE-EVs maintained relatively normal mitochondrial morphology including displaying elongated, rod-shaped structures with improved cristae and membrane integrity compared to both IL-1β and NC-EVs groups.

In summary, our results indicate that OE-EVs reprogrammed glycolytic metabolism in OA chondrocytes by inhibiting aerobic glycolysis and alleviating oxidative stress, while simultaneously improving mitochondrial morphology and function. Our findings indicate that

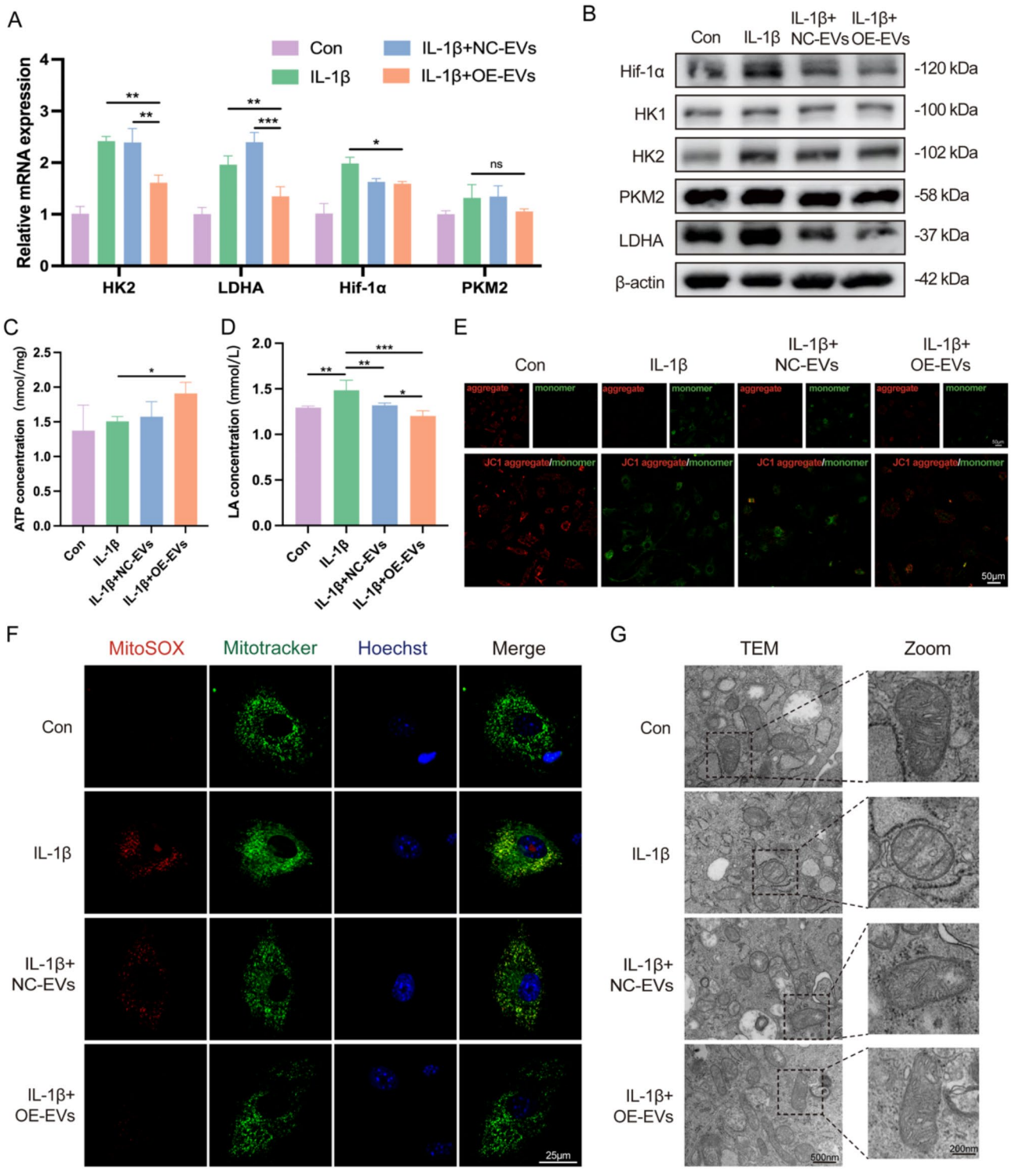

Fig. 4 OE-EVs reprogram metabolism in chondrocytes. (**A**&**B**) qRT-PCR and Western blot analysis of glycolytic enzyme expression. (**C**&**D**) ATP production and lactate levels in chondrocytes. (**E**) JC-1 staining of mitochondrial membrane potential (red: JC-1 aggregates, green: JC-1 monomers). (**F**) Mitochondrial ROS analysis using MitoSOX and Mitotracker staining. (**G**) TEM images of mitochondria in different groups. ($n = 3$, $^{*}p < 0.05$, $^{**}p < 0.01$, and $^{***}p < 0.001$)

Lacc1-enriched EVs regulate both chondrocyte metabolism and inflammation; however, whether Lacc1 itself plays a direct role in chondrocyte metabolic homeostasis remains unclear. Given that EV cargo exerts biological effects through intercellular communication, it is possible that the observed metabolic changes are mediated via multiple signaling pathways rather than direct intracellular Lacc1 activity. Future studies involving direct overexpression or knockdown of Lacc1 in chondrocytes will be needed to determine its potential cell-autonomous function. Clarifying this mechanism will be essential for fully elucidating the therapeutic potential of Lacc1-based EV interventions in TMJOA.

RNA-Seq analysis of the impact of OE-EVs on glycolysis and inflammation in OA chondrocytes

To further explore the underlying mechanism behind the therapeutic effects of OE-EVs, transcriptomic analysis was performed. A heatmap (Fig. 5A) depicting differentially expressed genes (DEGs) in IL-1β and OE-EVs-treated groups revealed significant alterations in the expression of key regulators of glycolytic and inflammatory. Notably, in the IL-1β group, the expression of glycolytic genes, including HK2, Pfkfb3, and Eno3, was significantly upregulated, suggesting enhanced glycolytic metabolism (Fig. 5A). In contrast, OE-EVs treatment markedly downregulated the expression of these genes (Fig. 5A), indicating a potential role of OE-EVs in glycolytic reprogramming in chondrocytes.

Additionally, inflammatory genes, such as Cxcl5, Ccl2, Nfkbia, Tnfaip3, and IL6, were significantly downregulated in the OE-EVs group compared to the IL-1β group. This downregulation further supports the anti-inflammatory effects of OE-EVs in OA chondrocytes. Moreover, the expression of genes involved in ECM degradation, including MMP3 and Adamts18, was significantly reduced in the OE-EVs-treated group, suggesting that OE-EVs may play a role in restraining ECM breakdown in OA. In addition, the expression of JAK2, a key component of the JAK-STAT signaling pathway, was notably decreased following OE-EVs treatment, further suggesting that OE-EVs may modulate glycolysis and inflammation, while suppressing ECM degradation and promoting proteoglycan synthesis in OA chondrocytes.

To gain further insights into the biological processes underpinning these changes, Gene Ontology (GO) enrichment analysis was performed. As shown in Fig. 5C, the most significantly enriched GO terms included processes related to glycolytic metabolism, carbohydrate metabolism, ATP generation from ADP, extracellular matrix organization, and glycosaminoglycan binding. These findings highlight the potential of OE-EVs in regulating metabolic processes and maintaining ECM homeostasis in OA.

In support of these results, Kyoto Encyclopedia of Genes and Genomes (KEGG) pathway analysis (Fig. 5B) identified several enriched pathways, including HIF-1 signaling, glycolysis/gluconeogenesis, TNF signaling, and JAK-STAT signaling. These pathways are consistent with OE-EVs' role in modulating glycolytic metabolism and inflammation. In addition, Gene Set Enrichment Analysis (GSEA) revealed notable variations in JAK-STAT signaling pathway and extracellular matrix (Fig. 5D), TNF signaling pathway and cell adhesion (Fig. S6). Compared to the IL-1β group, the enrichment of genes associated with extracellular matrix and cell adhesion was significantly increased in the OE-EVs group, meanwhile the genes relating to JAK-STAT and TNF signaling pathway displayed a significant decrease in the OE-EVs group. These results suggest that OE-EVs not only promote ECM synthesis but also inhibit the inflammatory response, likely through modulation of the JAK-STAT signaling pathway.

Previous studies have shown that pro-inflammatory cytokines (such as IL-1β, IL-6) and matrix metalloproteinase (MMP) activate the Janus Kinase/Signal Transducers and Activators of Transcription (JAK/STAT) signaling pathway, contributing to inflammation and cartilage degradation in OA. Inhibition of the JAK-STAT pathway has been shown to alleviate chondrocyte inflammation and protect against cartilage degeneration [43, 44]. To further verify the correlation between anti-inflammation effects of OE-EVs with regulating JAK-STAT signaling, we performed western blot analysis. As shown in Fig. 5E and F, the levels of phosphorylated JAK2 (p-JAK2) and STAT3 (p-STAT3), markers of JAK-STAT activation, as well as the ratios of p-JAK2/JAK2 and p-STAT3/STAT3, were significantly reduced in the OE-EVs group compared to the IL-1β group. These results indicate that OE-EVs exert inhibitory effects on the JAK-STAT pathway, thereby suppressing inflammation in OA chondrocytes.

In summary, our findings suggest that OE-EVs play an active role in regulating inflammation microenvironment of TMJOA. By reprogramming glycolysis, inhibiting key inflammatory pathways (including JAK-STAT, TNF, and HIF-1 signaling), and promoting ECM synthesis, OE-EVs help create a favorable microenvironment for chondrocyte function and protect against cartilage degradation.

OE-EVs alleviate inflammation and promote cartilage repair in TMJOA in vivo

Building upon the promising in vitro results, the therapeutic effects of OE-EVs were further assessed in vivo using a surgical induced mouse model of TMJOA [45, 46]. As illustrated in Fig. 6A, treatments began two weeks after unilateral discectomy to allow for TMJOA development. Mice in TMJOA group received intra-articular injections of PBS, while the NC-EVs and OE-EVs groups

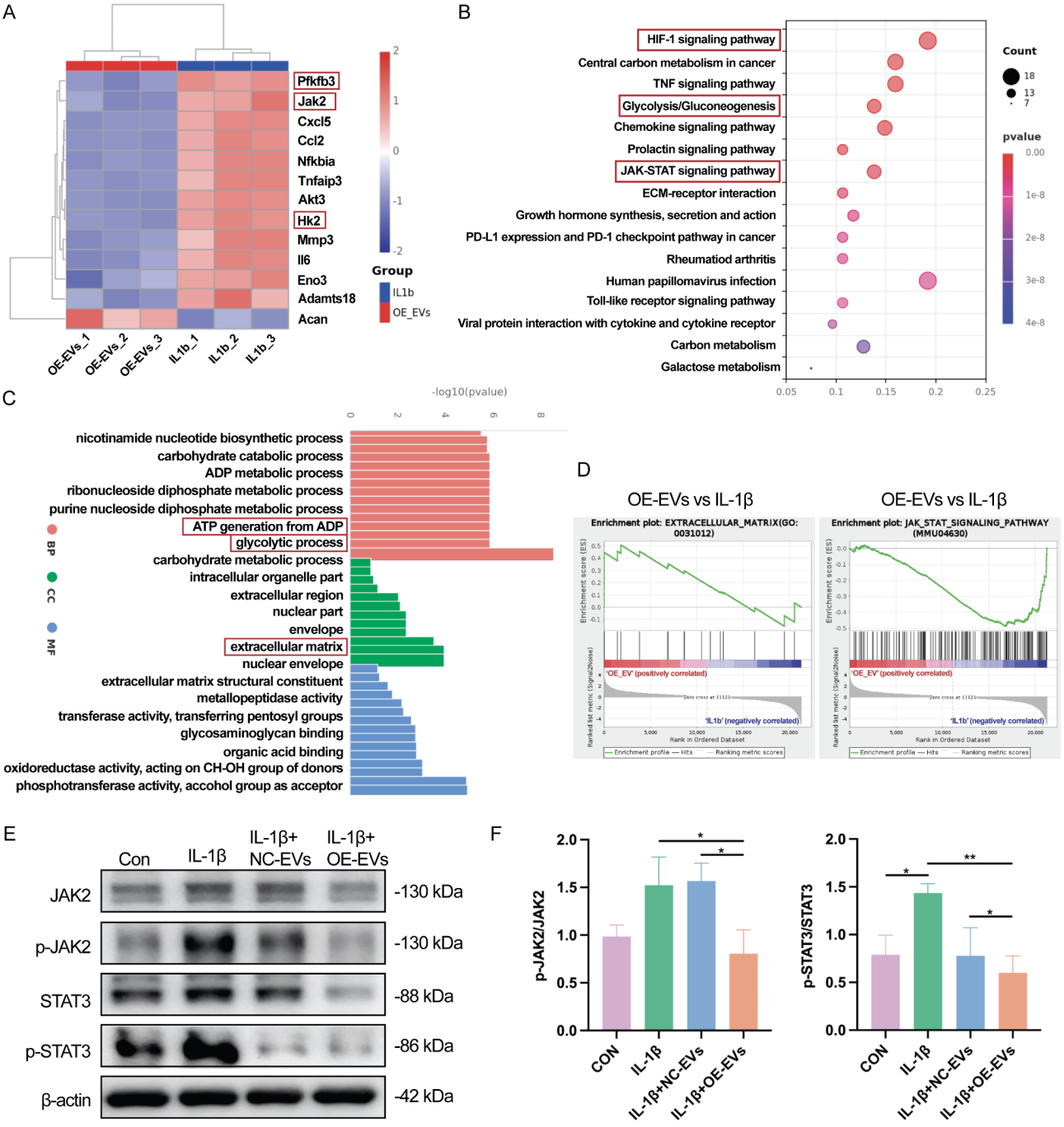

Fig. 5 Transcriptomic and signaling pathway analysis of IL-1β- and OE-EV-treated chondrocytes. (**A**) Heatmap of differentially expressed genes. (**B**&**C**) KEGG and GO enrichment analysis. (**D**) GSEA analysis of key pathways. (**E**&**F**) Western blot and semi-quantification of JAK-STAT signaling. ($n = 3$, $^{*}p < 0.05$ and $^{**}p < 0.01$)

received NC-EVs and OE-EVs, respectively. Four weeks post-treatment, TMJ tissues were harvested for analysis.

To examine the retention ability of EVs in vivo, PKH26 labeled OE-EVs and NC-EVs were injected into the TMJ, and fluorescence signals were tracked using an in vivo imaging system (Berthold, Germany). Fig. 6B showed that both OE-EVs and NC-EVs were retained in the tissue for over 72 h. For assurance of the sustained effects of OE-EVs, intra-articular injection was administered twice weekly. TMJs were harvested after four weeks of treatment.

Since inflammation in TMJOA also leads to subchondral bone deterioration, we evaluate the therapeutic effects of OE-EVs on subchondral bone remodeling

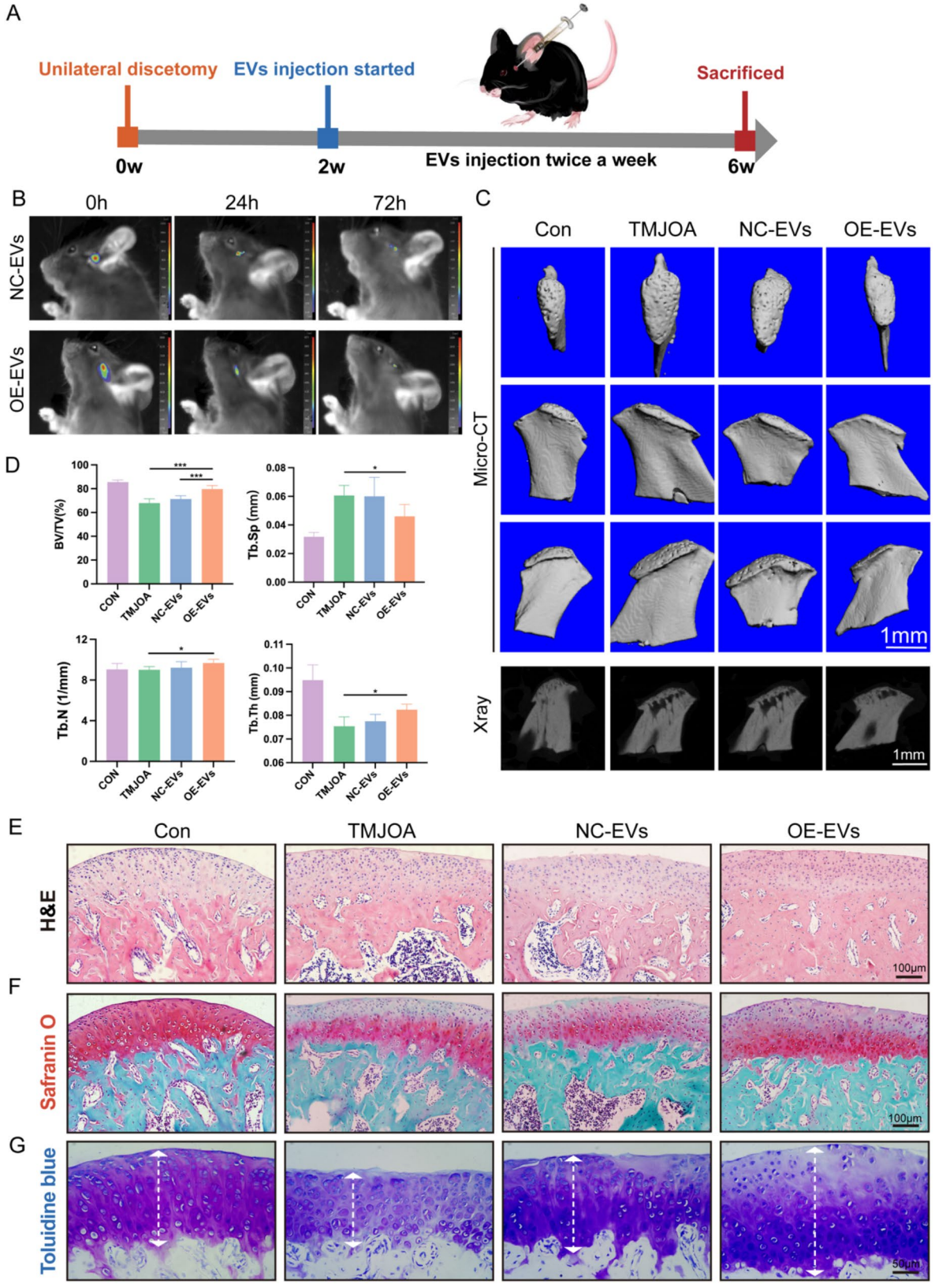

Fig. 6 OE-EVs promote cartilage repair and suppress inflammation in TMJOA in vivo. (**A**) Schematic of OE-EV treatment in a TMJ-OA mouse model. (**B**) In vivo fluorescence imaging of TMJ-injected OE-EVs and NC-EVs. (**C**&**D**) Micro-CT images and bone structural parameters. (**E**-**G**) Histological staining (H&E, Safranin O-Fast Green, Toluidine Blue). ($n = 6$, $^{*}p < 0.05$, and $^{***}p < 0.001$)

using Micro-CT and parametric analysis. The Micro-CT reconstruction images of condyle in Fig. 6C showed severe condylar cartilage and subchondral bone destruction including irregular trabecular structures and typical subchondral bone loss in the TMJOA group. In contrast, OE-EVs treatment notably preserved subchondral bone integrity, presenting a more regular trabecular pattern compared to the TMJOA and NC-EVs groups.

Subsequently, Bone structural parameters—including the ratio of bone volume to tissue volume (BV/TV), trabecular thickness (Tb.Th), trabecular number (Tb.N) and trabecular separation (Tb.Sp) were also examined. As shown in Fig. 6D, the TMJOA group had significantly lower BV/TV, Tb.Th, and Tb.N, along with increased Tb.Sp, indicating substantial bone structure deformation. OE-EVs treatment significantly improved BV/TV, Tb.Th, and Tb.N while reducing Tb.Sp, suggesting an effective amelioration of bone loss. No significant differences were observed between the TMJOA and NC-EVs groups. Thus, these results suggested that OE-EVs treatment effectively alleviated subchondral bone erosion caused by TMJOA and protected condylar subchondral bone structure.

OE-EVs exhibit excellent biocompatibility and do not cause systemic toxicity. To further assess the safety of OE-EVs in vivo, we performed H&E staining of major organs, including the heart, liver, spleen, lungs, and kidneys. The histological analysis (Fig. S7) revealed no detectable pathological abnormalities across all groups, indicating that OE-EV treatment does not induce observable toxicity or tissue damage. These findings, together with our in vitro CCK-8 and live/dead staining assays (Fig. S3), confirm that OE-EVs are well-tolerated and biocompatible, supporting their potential for clinical application.

Histological analysis was further conducted to evaluate changes in articular cartilage and subchondral bone. H&E staining (Fig. 6E) revealed characteristic TMJOA pathology in the TMJOA group, including disorganized cellular layers, a rough surface, inflammatory cells infiltration, and severe subchondral bone damage, whereas the OE-EVs group exhibited reduced TMJOA related histological alterations compared to the TMJOA and NC-EVs groups. Moreover, the Safranin O-fast green staining (Fig. 6F) was performed to assess the glycosaminoglycan (GAG) level deposited in cartilage, with TMJOA cartilage showing diminished and irregular Safranin O^+ matrix compared to the Con group. Notably, OE-EVs treatment resulted in a uniform and abundant distribution of the safranin O^+, suggesting enhanced GAG synthesis. Additionally, TB staining (Fig. 6G) revealed marked cartilage loss in the TMJOA group, while OE-EVs treatment preserved cartilage thickness, indicating effective protection against cartilage matrix degradation. Semi-quantitative analysis of toluidine blue-stained cartilage area in Fig. S8 showed a 1.55-fold increase in the OE-EV group compared to the TMJOA group, indicating enhanced proteoglycan accumulation. Previous study reported that EVs or engineered EVs restore TMJ condylar structure with amelioration in cell arrangement, cartilage thickness, cellularity and matrix synthesis and subchondral bone remodeling [47, 48]. Consistent with curative effects as previous work reported, OE-EVs treatment exhibited remarkable therapeutic effects in restoration of the TMJ condylar structure, including improvements in morphology and functional ingredients.

Collagen II and Aggrecan are essential for chondrogenesis, and their expression levels were evaluated by immunohistochemistry and immunofluorescence staining, respectively. Collagen II (Fig. 7A) and Aggrecan (Fig. 7C and F) expression was significantly suppressed in TMJOA group compared to the Con group. While OE-EVs markedly enhanced their expression, indicating that OE-EVs treatments effectively promote cartilage matrix regeneration and anabolic activity.

Moreover, inflammatory cytokines (such as IL-1β) and matrix metalloproteinases (MMP3, MMP9, MMP13) played pivotal roles in cartilage matrix degradation. Herein, the impact of OE-EVs on alleviating cartilage inflammation was investigated by immunohistochemical staining for IL-β (Fig. 7B) and immunofluorescence staining for MMP13 (Fig. 7D and G) and MMP3 (Fig. 7E and H). As the results showed, the expression of these proteins was significantly elevated in the TMJOA group; however, OE-EVs treatment effectively reduced IL-1β, MMP3 and MMP13 levels, demonstrating that OE-EVs significantly suppress catabolic and pro-inflammatory factors. As Fig. 7I showed, histological analysis was conducted using the OA Research Society International (OARSI) scoring system. The OE-EVs group displayed a significantly lower score compared to the TMJOA group, indicating a substantial therapeutic effect in mitigating OA-related damage.

We also conducted immunofluorescence staining of iNOS and Arg1 to verify the anti-inflammatory effects of OE-EVs in vivo. As Fig. S9 showed, these results demonstrated that in the OE-EV-treated group, Arg1 expression was upregulated, whereas iNOS expression was significantly reduced. This suggests that OE-EVs may mitigate TMJOA inflammation by promoting macrophage polarization toward an anti-inflammatory M2 phenotype, further supporting their therapeutic potential in modulating the joint microenvironment.

Based on the above results, OE-EVs exhibited favorable therapeutic potential by attenuating inflammation, enhancing cartilage regeneration, rebalancing cartilage anabolism and catabolism, preventing cartilage matrix degradation, and remodeling subchondral bone. Overall,

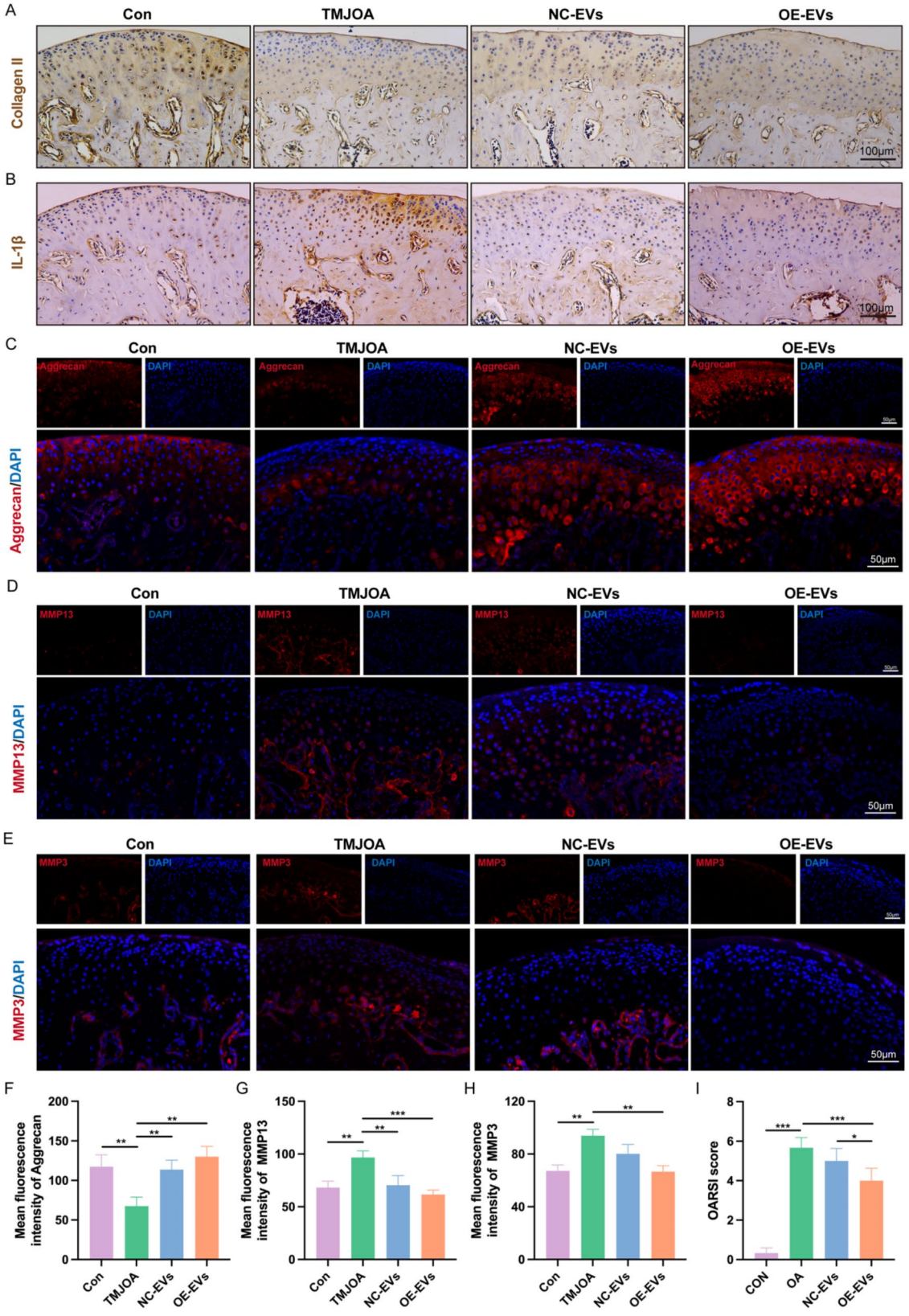

Fig. 7 Histological and immunohistochemical analysis of TMJ condyle tissue. (**A**&**B**) Immunohistochemical staining for Collagen II and IL-1β. (**C**-**E**) Immunofluorescence staining of Aggrecan, MMP13, and MMP3. (**F**-**H**) Quantification of fluorescence intensity. (**I**) OARSI scoring for cartilage degradation. ($n = 3$, $^{**}p < 0.01$, and $^{***}p < 0.001$)

OE-EVs successfully promoted cartilage repair and alleviated TMJOA inflammation progression in vivo.

While our 4-week data demonstrate the capacity of OE-EVs to mitigate early-stage TMJOA inflammation, chronic disease modification requires evaluation over extended periods (≥8 weeks). Future studies will optimize dosing schedules and incorporate longitudinal imaging (e.g., in vivo micro-CT) to track OA progression dynamically. This is critical for clinical translation, as TMJOA therapies must demonstrate durability beyond acute symptom relief.

While our TMJOA animal model offers valuable insights into disease mechanisms, it may not fully replicate the complexity of human TMJOA. Notably, anatomical and physiological differences exist between species, and animal models often simulate only specific aspects of the human condition [4]. Additionally, the long-term safety and stability of engineered extracellular vesicles (OE-EVs) remain areas requiring further investigation. Factors such as optimal storage conditions and potential immunogenic responses need to be thoroughly evaluated to ensure their viability as therapeutic agents.

Conclusion

This study identifies significant metabolic dysregulation in TMJOA chondrocytes and demonstrates the therapeutic potential of Lacc1-engineered extracellular vesicles (OE-EVs) as a metabolic intervention. By restoring metabolic balance, OE-EVs markedly suppress IL-1β-induced inflammation and improve mitochondrial function, as evidenced by reduced lactate production, decreased mitochondrial superoxide levels, and normalization mitochondrial structure. In vivo, OE-EV treatment not only alleviates inflammation but also enhances cartilage regeneration in TMJOA models. These findings highlight a novel therapeutic approach targeting chondrocyte metabolism, providing a promising strategy for TMJOA management with potential clinical applications. Moving forward, additional studies are warranted to elucidate the mechanistic pathways underlying Lacc1-mediated metabolic reprogramming, as well as to assess the long-term efficacy and safety of OE-EVs, thereby facilitating clinical translation.

Supplementary Information

The online version contains supplementary material available at https://doi.org/10.1186/s12951-025-03355-5.

Supplementary Material 1

Author contributions

JX designed the study, JX and JS supervised the study; XH and JX performed the experiments, analyzed the data, wrote and revised the manuscript; JS provided administrative and material support. All authors read and approved the final manuscript.

Funding

The authors gratefully acknowledge the support of the National Natural Science Foundation of China (81873715, 82170913), China Postdoctoral Science Foundation (2023M742645), Science and Technology Commission of Shanghai Municipality (23YF1450400, 201409006200).

Data availability

No datasets were generated or analysed during the current study.

Author information

Ethics approval and consent to participate

All animal experimental protocols were approved by Animal Welfare Committee of Stomatological Hospital of Tongji University (Approved No. 2024-DW-19).

Consent for publication

Not applicable.

Competing interests

The authors declare no competing interests.

Author details

[1]Shanghai Engineering Research Center of Tooth Restoration and Regeneration & Tongji Research Institute of Stomatology & Department of Prosthodontics, Dental School, Shanghai Tongji Stomatological Hospital, Tongji University, Shanghai 200072, China

Received: 11 December 2024 / Accepted: 24 March 2025
Published online: 05 April 2025

References

1. Wang XD, Zhang JN, Gan YH, Zhou YH. Current Understanding of pathogenesis and treatment of TMJ osteoarthritis. J Dent Res. 2015;94:666–73.
2. Lu K, Ma F, Yi D, Yu H, Tong L, Chen D. Molecular signaling in temporomandibular joint osteoarthritis. J Orthop Translat. 2022;32:21–7.
3. Delpachitra SN, Dimitroulis G. Osteoarthritis of the temporomandibular joint: a review of aetiology and pathogenesis. Br J Oral Maxillofac Surg. 2022;60:387–96.
4. Wang D, Qi Y, Wang Z, Guo A, Xu Y, Zhang Y. Recent advances in animal models, diagnosis, and treatment of temporomandibular joint osteoarthritis. Tissue Eng Part B. 2023;29:62–77.
5. Derwich M, Mitus-Kenig M, Pawlowska E. Orally administered NSAIDs-General characteristics and usage in the treatment of temporomandibular joint Osteoarthritis-A narrative review. Pharmaceuticals (Basel). 2021;14:219.
6. Li B, Guan G, Mei L, Jiao K, Li H. Pathological mechanism of chondrocytes and the surrounding environment during osteoarthritis of temporomandibular joint. J Cell Mol Med. 2021;25:4902–11.
7. Wu Z, Wang Y, Zhu M, Lu M, Liu W, Shi J. Synovial microenvironment in temporomandibular joint osteoarthritis: crosstalk with chondrocytes and potential therapeutic targets. Life Sci. 2024;354:122947.
8. Cisewski SE, Zhang L, Kuo J, Wright GJ, Wu Y, Kern MJ, Yao H. The effects of oxygen level and glucose concentration on the metabolism of Porcine TMJ disc cells. Osteoarthritis Cartilage. 2015;23:1790–6.
9. Zheng L, Zhang Z, Sheng P, Mobasheri A. The role of metabolism in chondrocyte dysfunction and the progression of osteoarthritis. Ageing Res Rev. 2021;66:101249.
10. Wu X, Liyanage C, Plan M, Stark T, McCubbin T, Barrero RA, Batra J, Crawford R, Xiao Y, Prasadam I. Dysregulated energy metabolism impairs chondrocyte function in osteoarthritis. Osteoarthritis Cartilage. 2023;31:613–26.
11. Defois A, Bon N, Charpentier A, Georget M, Gaigeard N, Blanchard F, Hamel A, Waast D, Armengaud J, Renoult O, et al. Osteoarthritic chondrocytes undergo a glycolysis-related metabolic switch upon exposure to IL-1b or TNF. Cell Commun Signal. 2023;21:137.
12. Papatriantafyllou M. PDZK1 downregulation linked to mitochondrial dysfunction in OA. Nat Rev Rheumatol. 2024;20:597.
13. Sanchez-Lopez E, Coras R, Torres A, Lane NE, Guma M. Synovial inflammation in osteoarthritis progression. Nat Rev Rheumatol. 2022;18:258–75.

14. Zhao K, Ruan J, Nie L, Ye X, Li J. Effects of synovial macrophages in osteoarthritis. Front Immunol. 2023;14:1164137.
15. Wang WY, Chu YR, Zhang PY, Liang Z, Fan ZL, Guo XQ, Zhou GD, Ren WJ. Targeting macrophage polarization as a promising therapeutic strategy for the treatment of osteoarthritis. Int Immunopharmacol. 2023;116:109790.
16. Peng S, Yan Y, Li R, Dai H, Xu J. Extracellular vesicles from M1-polarized macrophages promote inflammation in the temporomandibular joint via miR-1246 activation of the Wnt/beta-catenin pathway. Ann N Y Acad Sci. 2021;1503:48–59.
17. Kim H, Back JH, Han G, Lee SJ, Park YE, Gu MB, Yang Y, Lee JE, Kim SH. Extracellular vesicle-guided in situ reprogramming of synovial macrophages for the treatment of rheumatoid arthritis. Biomaterials. 2022;286:121578.
18. Liu Z, Zhuang Y, Fang L, Yuan C, Wang X, Lin K. Breakthrough of extracellular vesicles in pathogenesis, diagnosis and treatment of osteoarthritis. Bioact Mater. 2023;22:423–52.
19. Kalluri R, LeBleu VS. The biology, function, and biomedical applications of exosomes. Science. 2020;367:eaau6977.
20. de Abreu RC, Fernandes H, Martins PAD, Sahoo S, Emanueli C, Ferreira L. Native and bioengineered extracellular vesicles for cardiovascular therapeutics. Nat Rev Cardiol. 2020;17:685–97.
21. Wei Z, Oh J, Flavell RA, Crawford JM. LACC1 bridges NOS2 and polyamine metabolism in inflammatory macrophages. Nature. 2022;609:348–53.
22. Lahiri A, Hedl M, Yan J, Abraham C. Human LACC1 increases innate receptor-induced responses and a disease-risk variant modulates these outcomes. Nat Commun. 2017;8:15614.
23. Omarjee O, Mathieu AL, Quiniou G, Moreews M, Ainouze M, Frachette C, Melki I, Dumaine C, Gerfaud-Valentin M, Duquesne A, et al. LACC1 deficiency links juvenile arthritis with autophagy and metabolism in macrophages. J Exp Med. 2021;218:e20201006.
24. Cader MZ, Boroviak K, Zhang Q, Assadi G, Kempster SL, Sewell GW, Saveljeva S, Ashcroft JW, Clare S, Mukhopadhyay S, et al. C13orf31 (FAMIN) is a central regulator of immunometabolic function. Nat Immunol. 2016;17:1046–56.
25. Bao C, Zhu S, Song K, He C. HK2: a potential regulator of osteoarthritis via glycolytic and non-glycolytic pathways. Cell Commun Signal. 2022;20:132.
26. Ranjan P, Sarma M, Dubey VK. Biochemical and biophysical characterization of citrate synthase. Int J Biol Macromol. 2024;279:135400.
27. Ait-El-Mkadem S, Dayem-Quere M, Gusic M, Chaussenot A, Bannwarth S, Francois B, Genin EC, Fragaki K, Volker-Touw CLM, Vasnier C, et al. Mutations in MDH2, encoding a Krebs cycle enzyme, cause Early-Onset severe encephalopathy. Am J Hum Genet. 2017;100:151–59.
28. Cao K, Xu J, Cao WL, Wang XQ, Lv WQ, Zeng MQ, Zou X, Liu JK, Feng ZH. Assembly of mitochondrial succinate dehydrogenase in human health and disease. Free Radical Biol Med. 2023;207:247–59.
29. Arra M, Swarnkar G, Ke K, Otero JE, Ying J, Duan X, Maruyama T, Rai MF, O'Keefe RJ, Mbalaviele G, et al. LDHA-mediated ROS generation in chondrocytes is a potential therapeutic target for osteoarthritis. Nat Commun. 2020;11:3427.
30. Yang XB, Chen WP, Zhao X, Chen LW, Li WL, Ran JS, Wu LD. Pyruvate kinase M2 modulates the Glycolysis of chondrocyte and extracellular matrix in osteoarthritis. DNA Cell Biol. 2018;37:271–77.
31. Auger JP, Zimmermann M, Faas M, Stifel U, Chambers D, Krishnacoumar B, Taudte RV, Grund C, Erdmann G, Scholtysek C, et al. Metabolic rewiring promotes anti-inflammatory effects of glucocorticoids. Nature. 2024;629:184–92.
32. Choo YW, Kang M, Kim HY, Han J, Kang S, Lee JR, Jeong GJ, Kwon SP, Song SY, Go S, et al. M1 Macrophage-Derived nanovesicles potentiate the anticancer efficacy of immune checkpoint inhibitors. ACS Nano. 2018;12:8977–93.
33. Yang J, Li SS, Li ZY, Yao LT, Liu MJ, Tong KL, Xu QT, Yu B, Peng R, Gui T, et al. Targeting YAP1-regulated Glycolysis in Fibroblast-Like synoviocytes impairs macrophage infiltration to ameliorate diabetic osteoarthritis progression. Adv Sci. 2024;11:e2304617.
34. Khatri M, Richardson LA, Meulia T. Mesenchymal stem cell-derived extracellular vesicles attenuate influenza virus-induced acute lung injury in a pig model. Stem Cell Res Ther. 2018;9:17.
35. Chen C, Cai N, Niu Q, Tian Y, Hu Y, Yan X. Quantitative assessment of lipophilic membrane dye-based labelling of extracellular vesicles by nano-flow cytometry. J Extracell Vesicles. 2023;12:e12351.
36. Aisenbrey EA, Bryant SJ. The role of chondroitin sulfate in regulating hypertrophy during MSC chondrogenesis in a cartilage mimetic hydrogel under dynamic loading. Biomaterials. 2019;190:51–62.
37. Rolvien T, Yorgan TA, Kornak U, Hermans-Borgmeyer I, Mundlos S, Schmidt T, Niemeier A, Schinke T, Amling M, Oheim R. Skeletal deterioration in-related spondyloepiphyseal dysplasia occurs prior to osteoarthritis. Osteoarthr Cartil. 2020;28:334–43.
38. Zhou HQ, Mu YL, Ma C, Zhang Z, Tao C, Wang DA. Rejuvenating hyaline cartilaginous phenotype of dedifferentiated chondrocytes in collagen II scaffolds: A mechanism study using chondrocyte membrane nanoaggregates as antagonists. ACS Nano. 2024;18:2077–90.
39. Tianyuan Z, Haoyuan D, Jianwei L, Songlin H, Xu L, Hao L, Zhen Y, Haotian D, Peiqi L, Xiang S, et al. A smart MMP13-Responsive injectable hydrogel with inflammatory diagnostic logic and multiphase therapeutic ability to orchestrate cartilage regeneration. Adv Funct Mater. 2023;33:2213019.
40. Zhang SP, Teo KYW, Chuah SJ, Lai RC, Lim SK, Toh WS. MSC exosomes alleviate temporomandibular joint osteoarthritis by attenuating inflammation and restoring matrix homeostasis. Biomaterials. 2019;200:35–47.
41. Qian Y, Chu G, Zhang L, Wu Z, Wang Q, Guo JJ, Zhou F. M2 macrophage-derived Exosomal miR-26b-5p regulates macrophage polarization and chondrocyte hypertrophy by targeting TLR3 and COL10A1 to alleviate osteoarthritis. J Nanobiotechnol. 2024;22:72.
42. Lin R, Yin J, Huang J, Zou L, Liu L, Tang W, Zhang H, Yang L, Zhang Y, Li G, et al. Macrophage-derived ectosomal miR-350-3p promotes osteoarthritis progression through downregulating chondrocyte H3K36 methyltransferase NSD1. Cell Death Discov. 2024;10:223.
43. Raychaudhuri SP, Shah RJ, Banerjee S, Raychaudhuri SK. JAK-STAT signaling and beyond in the pathogenesis of spondyloarthritis and their clinical significance. Curr Rheumatol Rep. 2024;26:204–13.
44. Sims NA. The JAK1/STAT3/SOCS3 axis in bone development, physiology, and pathology. Exp Mol Med. 2020;52:1185–97.
45. Wu W, Hu A, Xu H, Su J. LincRNA-EPS alleviates inflammation in TMJ osteoarthritis by binding to SRSF3. J Dent Res. 2023;102:1141–51.
46. Kamikawatoko T, Yotsuya M, Owada A, Ishizuka S, Kasahara M, Yamamoto M, Abe S, Sekine H. Early changes in Asporin levels in osteoarthritis of the temporomandibular joint. J Oral Biosci. 2024;66:546–53.
47. Zhu Y, Cao LY, Yuan M, Chen XZ, Xie XR, Li MH, Yang C, Wang XS, Ma ZG. Microgel encapsulated mesoporous silica nanoparticles for releasing Wnt16 to synergistically treat temporomandibular joint osteoarthritis. Adv Sci. 2024;11:e2404396.
48. Liao SN, Liu ZQ, Lv WT, Li SH, Tian TR, Wang YF, Wu HY, Zhao ZH, Lin YF. Efficient delivery of SiRNA via tetrahedral framework nucleic acids: inflammation Attenuation and matrix regeneration in temporomandibular joint osteoarthritis. ACS Appl Mater Interfaces. 2024;16:53499–514.

Publisher's note